Asian Journal of Chemistry; Vol. 36, No. 10 (2024), 2423-2430

ASIAN JOURNAL OF CHEMISTRY

https://doi.org/10.14233/ajchem.2024.31250

Synthesis and Characterization of CuO Nanoparticles from *Kappaphycus alvarezii* Derived Carrageenan for the Photocatalytic Degradation of Methylene Blue Dye

JERIN JAMES[1], NISHESH SHARMA[1], PRIYVART CHOUDHARY[2], AMIT SEMWAL[3], ROHIT SHARMA[4,*] and VINAY DIWEDI[5]

[1]Department of Biotechnology, School of Applied and Lifesciences, Uttaranchal University, Dehradun-248007, India
[2]Research & Development Cell, Biotechnology Department, Manav Rachna International Institute of Research and Studies (Deemed to be University) Faridabad-121004, India
[3]College of Pharmacy, Shivalik Campus, Dehradun-248197, India
[4]Department of Biotechnology Engineering and Food Technology, University Institute of Engineering, Chandigarh University, Chandigarh-140413, India
[5]Amity Institute of Biotechnology, Amity University, Gwalior-474005, India

*Corresponding author: E-mail: rohit.e15684@cumail.in

Received: 30 November 2023; *Accepted*: 16 September 2024; *Published online*: 30 September 2024; AJC-21774

The present study investigates the synthesis and characterization of copper oxide (CuO) nanoparticles embedded in carrageenan matrices derived from green and brown strains of *Kappaphycus alvarezii*. The CuO-carrageenan nanoparticles (CuO-CRGg and CuO-CRGb) exhibit distinct absorption peaks at 295 nm and 301 nm, respectively suggesting variations in particle size distribution and crystallinity. Morphological analysis through SEM reveals the agglomerated structures with average particle sizes of 93 nm for CuO-CRGg and 106 nm for CuO-CRGb. FTIR analysis indicates the presence of functional groups including 3,6-anhydrogalactose from carrageenan, whereas the XRD analysis shows the average crystalline sizes of 26 nm and 27 nm for CuO-CRGg and CuO-CRGb, respectively. The energy levels associated with CuO-CRGg and CuO-CRGb nanoparticles are confirmed with a characteric peak at 4.20 and 4.12 eV, respectively suggesting wide bandgap semiconductor properties. The CuO-CRGb nanoparticles demonstrate higher photocatalytic efficiency under UV light (89.76%) compared to visible light (55.21%), with rate constants of 0.035 min^{-1} and a half-life of 4.04 min. Whereas CuO-CRGg nanoparticles exhibit efficiencies of 86.87% under UV light and 64.38% under visible light, with a rate constant of 0.033 min^{-1} and a half-life of 4.12 min under UV light and 0.011 min^{-1} and a half-life of 5.15 min under visible light.

Keywords: Carrageenan nanoparticles, *Kappaphycus alvarezii*, CuO nanoparticles, Photocatalysis, Methylene blue degradation.

INTRODUCTION

Biopolymeric nanoparticles are intricate nanostructures that originate from polymers sourced from natural resources such as plant extracts, marine organisms and microbial sources. These biopolymeric nanoparticles find applications across various fields, including medicine, agriculture and environmental science, capitalizing on their unique properties and the renewable nature of their source materials [1]. These nanoparticles derived from biopolymers can be customized and designed to envelop, shield and transport an extensive array of therapeutic substances, encompassing medications, proteins and genetic material. Due to their biocompatibility and inherent affinity to biological systems, they hold significant potential in biomedical fields such as drug delivery, tissue engineering and diagnostics [2,3].

The use of biopolymers like carrageenan, cellulose and chitosan in nanoparticle synthesis ensures that these nanoparticles are not only functional but also environmental friendly [4]. Carrageenan biopolymer nanoparticles are constructed using carrageenan, a natural polysaccharide extracted from various species of red seaweed. The present study focuses on the therapeutic potential of the nanoparticle synthesized from crude carrageenan extracted from different colour strains (green and brown) of *Kappaphycus alvarezii.* Nanoparticles synthesized from *Kappaphycus alvarezii*, red algae belongs to the family *Areschougiaceae* within the order *Gigartinales* offers distinct advantages due to their abundance, sustainability, biocompati-

bility and potential for controlled synthesis. *Kappaphycus alvarezii* exists in both green and brown strains, each possessing distinct physiological and biochemical traits that influence their potential applications in various fields [5]. Compounds derived from *K. alvarezii* exhibit natural biocompatibility and biodegradability, making them suitable for eco-friendly nanoparticle production [6,7]. These compounds contain functional groups that aid in nanoparticle stabilization and controlled growth [8].

Carrageenan nanocomposites emerge through the integration of metallic nanoparticles into carrageenan hydrogels commonly composed of prevalent metals like gold, silver, iron, copper, platinum and zinc [9]. CuO nanoparticles synthesized sustainably exhibit diverse applications, particularly in photocatalysis. Employing green methods, they enhance sensitivity and selectivity in electrochemical sensors for detecting pollutant dyes. Their distinctive properties, including efficient electron transfer and high surface area, contribute to the improved performance of the sensor [10]. The nanoparticles have been reported to exhibit enhancement in antimicrobial activity, magnetic manipulation, catalysis and imaging [11]. Moreover, metal oxide integration contributes not only to advancing medical and technological fields but also to the progression of environmentally conducive photocatalytic processes [12]. Recent investigations have revealed the potential for synergistic enhancement in the efficiency of photocatalytic degradation processes that focus on organic dyes.

Photocatalysis harnesses semiconducting materials as catalysts, utilizing their capacity to generate electron-hole pairs upon absorbing photons. The subsequent movement of these charge carriers to the material's surface facilitates redox reactions guiding the transformation of pollutants into less harmful forms [13]. This photo-induced transformation aligns closely with the principles of green chemistry and embodies the spirit of environmentally conscious innovation. Within potential pollutants, methylene blue serves as a representative target for assessing the effectiveness of photocatalytic processes [14]. As an organic dye widely used in various applications, its molecular structure allows for easy degradation under photocatalytic conditions. The transformation of methylene blue highlights the power of photocatalysis in breaking down complex chemical bonds and establishes a crucial framework for assessing the kinetics and mechanisms of such reactions [15]. This research not only sheds light on the promising applications of copper oxide nanoparticles synthesized from *K. alvarezii* derived carrageenan but also underscores the pivotal role of innovative photocatalytic approaches in addressing the environmental pollutants. The present study explores a novel approach to synthesize CuO nanoparticles has emerged through the green synthesis method utilizing extracts from *K. alvarezii*. This innovative technique offers an environmental friendly alternative to conventional methods, exhibiting the potential of natural resources in nanoparticle fabrication. Utilizing these newly synthesized CuO nanoparticles can lead to the substantial progress in photocatalysis applications, offering promising opportunities for sustainable material development and environmental remediation techniques.

EXPERIMENTAL

Kappaphycus alvarezii seaweed samples were purchased from a commercial farm site in Mandapam, India. The collected seaweed biomass underwent a process of removing unwanted debris, followed by the separation of the green and brown colour strains. Subsequently, both types of seaweed were sun-dried for a period of 5-10 days. After the drying process, the resulting material was transported to the laboratory for carrageenan extraction. The dried seaweeds were first rinsed in water and then oven-dried overnight. The oven-dried green and brown seaweeds were then milled to facilitate the subsequent steps of producing crude Carrageenan. The specified amount of milled seaweed samples was soaked for 30 min and subjected to a 10% KOH treatment for 2 h at 60 ± 3 ºC. The resulting colloidal solution was filtered using nylon sheets to eliminate solid residue. The solution obtained after filtration underwent a precipitation reaction with 0.05 N HCl to isolate the carrageenan extract. The precipitated carrageenan was washed through centrifugation to maintain neutral pH and the extracted gel was utilized for nanoparticle synthesis. The CuO nanoparticles were synthesized using the sol-gel method, employing 1 M $CuSO_4$ mixed with carrageenan gel at a 1:5 ratio for 3 h. The colour change in the solution, subsequent to the addition of carrageenan, was sustained for 1 h. Following this, 1 N NaOH was added dropwise, resulting in a subsequent colour change that persisted for 2 h. The obtained solution was washed with distilled water and ethanol to eliminate impurities, achieved through centrifugation. Subsequently, the solution underwent annealed at 400 ºC followed by oven drying.

The absorption spectrum of the analyzed nanoparticles was observed using a UV-VIS spectrophotometer (Systronics AU-2701:India) across a wavelength range of 200-800 nm. Molecular analysis of the sample was conducted utilizing a Fourier transform infrared (FTIR) spectrometer (Nicolet Summit LITE iD1: USA). FTIR measurements were performed in the wavenumber range of 4000-400 cm^{-1} to investigate both the molecular composition and functional groups present within the sample. The morphology of the nanoparticles was examined through scanning electron microscopy using (ZEISS-EVO 60: German model). The structure of the compounds was probed through X-ray diffraction (XRD), employing Cu$K\alpha$ radiation. Additionally, EDX mapping was carried out to further analyze the elemental distribution within the sample.

The photocatalytic degradation of methylene blue dye was conducted using a 10 ppm of dye along with copper oxide-carrageenan nanoparticles derived from both green strain and brown strain of *K. alvarezii*. 2.5% copper oxide nanoparticles were added to 50 mL aqueous solution of methylene blue dye and the mixture was stirred magnetically in dark for 30 min. Subsequently, the solution was exposed to UV-visible sunlight for activation, while absorbance at 664 nm was continuously measured using a UV-VIS spectrophotometer for up to 90 min.

RESULTS AND DISCUSSION

UV-visible spectral studies: The CuO nanoparticles of carrageenan extracted green strain *Kappaphycus alvarezii* (CuO-

CRGg) and brown strain *K. alvarezii* (CuO-CRGb) exhibited absorption peak at 295 nm and 301 nm, respectively (Fig. 1). The observation reveals that CuO-CRGg nanoparticles display a broader and less intense absorption peak compared to CuO-CRGb nanoparticles, which exhibit a narrower and higher intensity peak. The differences suggest variations in particle size distribution, crystallinity and possibly aggregation. The broader peak of CuO-CRGg indicates a wider range of absorbed wavelengths, possibly due to diverse particle sizes or structural variations. In contrast, the narrower peak of CuO-CRGb suggests a more uniform size distribution and well-defined absorption behaviour. The absorption spectra of the copper oxide nanoparticles were observed within the 250-300 nm range, with the extent of absorption being influenced by the size and morphology of the synthesized nanoparticles [16]. The presence of an absorption peak in the UV region of the electromagnetic spectrum suggests that the material is absorbing high-energy light. This absorption often indicates electronic transitions within the material, involving valence electrons moving to higher energy levels or transferring between energy bands [17]. The present study also revealed that the energy levels associated with CuO-CRGg and CuO-CRGb nanoparticles are characterized by a significant peak of 4.20 and 4.12 eV. Such a peak energy value suggests that CuO nanoparticles possess a distinctive electronic behaviour, making them a wide bandgap semiconductor material [18,19]. These materials have demonstrated the capacity for effective photocatalytic degradation processes.

Morphological studies: SEM analysis of synthesized CuO-Carrgaeenan nanoparticles clustered together to form agglomerated structures. The nanoparticles prepared from green strain *K. alvarezii* (CuO-CRGg) and brown strain *K. alvarezii* (CuO-CRGb) exhibits average particle size of 93 nm and 106 nm, respectively (Fig. 2). CuO nanoparticles typically have a size range of 80 to 100 nm, which holds significance due to the potential for unique properties stemming from the small size and increased surface area [20]. Generally, KCl is introduced as a crosslinking agent [21] and the studies reported that incorporation of soluble salts like KCl in carrageenan based materials preparation make the nanoparticle surface rough and less homogenized [22]. In current study, the surface of both nanoparticles found to be smooth and homogenized as KCl wasn't used. The nanoparticles with smooth and homogenized surface areas offer benefits include enhanced reactivity, uniform dispersion, improved optical and electronic properties, biocompatibility and targeted delivery potential [23].

Elemental analysis by EDX: The EDX analysis of CuO nanoparticles (CuO-CRGg and CuO-CRGb) was conducted at energy level of 20 keV (Fig. 3). The results revealed the dispersion energies of copper (Cu) and oxygen (O) at 0.998 keV and 0.654 keV, respectively. The weight percentages of oxygen and copper elements in the CuO-CRGg and CuO-CRGb nanoparticles were 9.0%, 87.3% and 13.3%, 82.1%, respectively. Both synthesized nanoparticles contain the elements nearly in stochiometric ratios but CuO-CRGb contains relatively more near to validates the presence of CuO nanoparticles. But, CuO-CRGg posses a stochiometric ratio of 1.55 nearly validate the presence of CuO nanoparticles. Similarly, in another study conducted by Tharani & Nehru [24] validated the indication of CuO nanoparticles in sample having ratio of 2.33 exhibit the photocatalytic degradation property under visible light with the degradation efficiency of 90% rhodamine dye. While comparing with the degradation efficiency, CuO-CRGb nanoparticles, which possess near ratio of 1:1 exhibit greater efficiency in photocatalysis. Analysis also found that nanoparticles were devoid of unwanted impurities and negligible presence of carbon content.

FTIR spectral studies: The CuO-carrageenan synthesized from brown strain (CuO-CRGb) and green strain (CuO-CRGg) provided FTIR spectrum with wavenumbers 3697.87 cm^{-1}, 3040.56 cm^{-1}, 2881.62 cm^{-1}, 2382 cm^{-1}, 1417 cm^{-1}, 1050.81 cm^{-1}; and 3620 cm^{-1}, 2884.62 cm^{-1}, 2825 cm^{-1}, 1426 cm^{-1} and 1040.81 cm^{-1}, respectively (Fig. 4). The wavenumbers 3620 cm^{-1} and 3697.87 cm^{-1} corresponds to the O-H stretching vibration of hydroxyl groups found in compounds like alcohols and phenols. The peak at 3040.558 cm^{-1} signifies the C-H stretching vibration of aromatic (benzene ring) [25], while the peak at 2382 cm^{-1} is associated with the peak at 1417 cm^{-1} observed in the fingerprint region, potentially indicating unique funct-

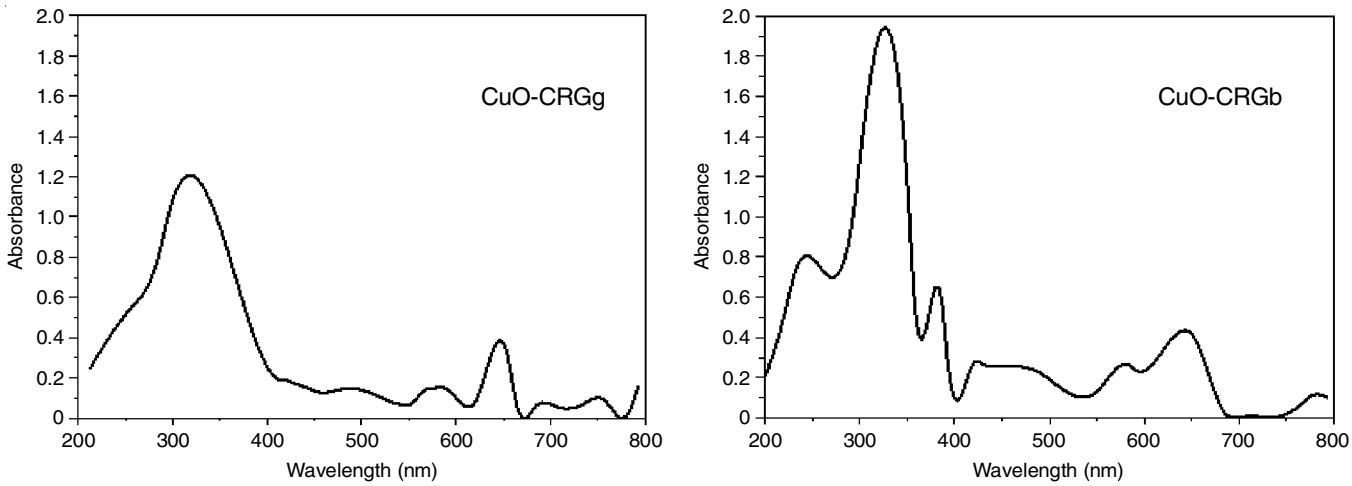

Fig. 1. UV-Vis absorption spectra of CuO nanocomposites synthesized using carrageenan (CuO-CRGg and CuO-CRGb), showing absorption peaks at 295 nm and 301 nm, respectively

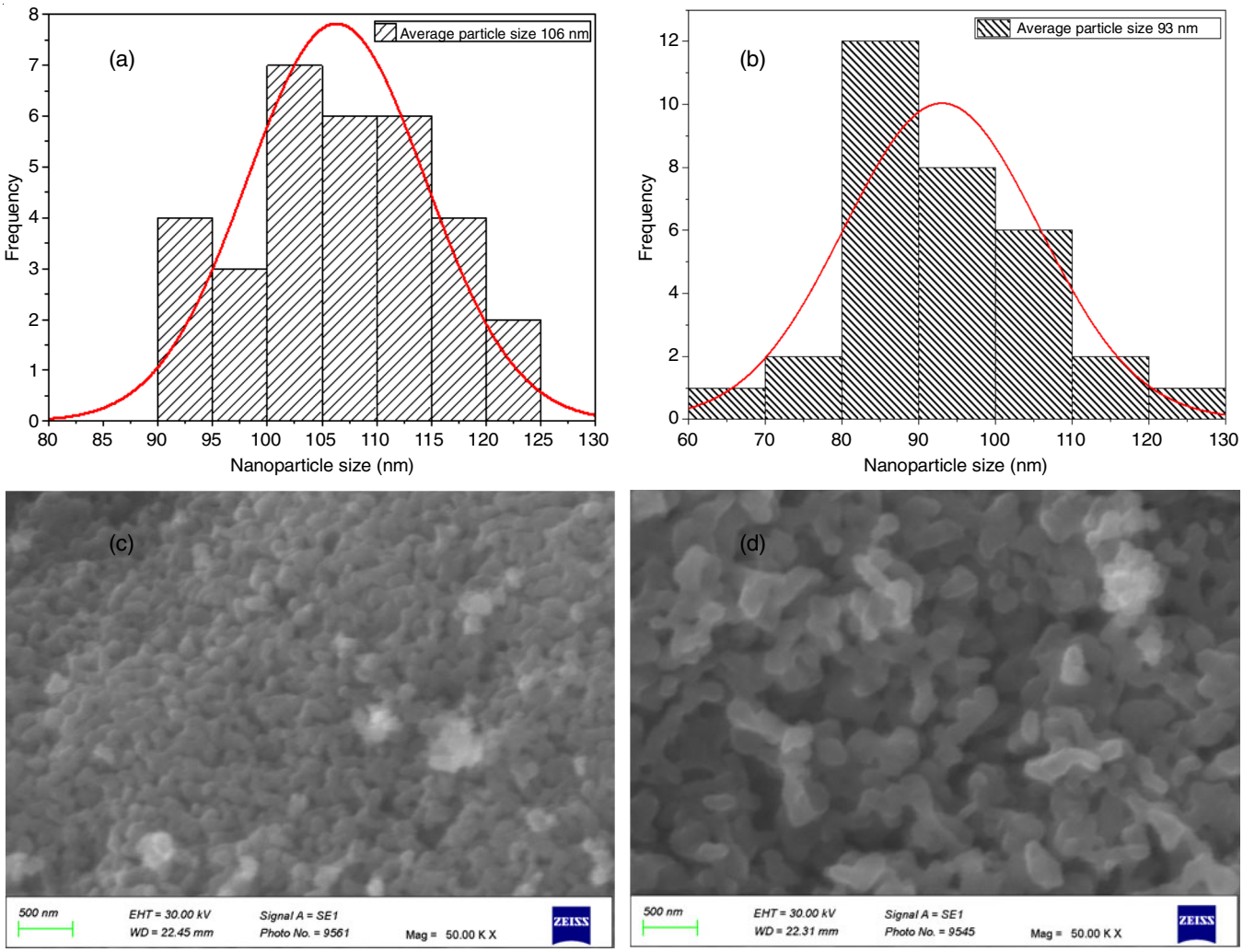

Fig. 2. (a) Frequency distribution graph of particle size ranging from 90-125 nm of CuO-CRGb, (b) Frequency distribution graph of particle size ranging from 60-130 nm of CuO-CRGg, (c) Electron microscopic image of synthesized CuO-CRGg with a scale of 500 nm and (d) Electron microscopic image of synthesized CuO-CRGb with a scale of 500 nm

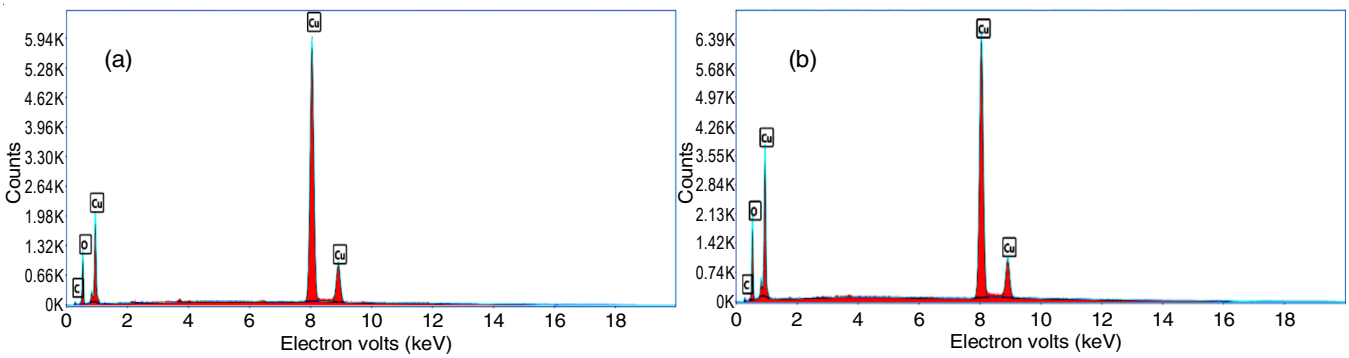

Fig. 3. Energy dispersive X-ray spectroscopic graph of (a) CuO-CRGg and (b) CuO-CRGb

ional groups or structural features. Significantly, the peaks at 1040.81 and 1050.81 cm^{-1} confirmed the presence of 3,6-anhydro-galactose, a constituent of carrageenan [26].

XRD spectral studies: The crystal structure examination of CuO-carrageenan nanoparticles derived from the green and brown strains of *Kappaphycus alvarezii* (CuO-CRGg and CuO-CRGb) were analyzed by XRD analysis. The calculation of the average crystalline size of CuO-carrageenan nanoparticles has been performed by Scherrer's equation (eqn. 1):

$$D = \frac{k\lambda}{\beta\cos\theta} \quad (1)$$

where D represents the average crystalline domain size; k is the Scherrer constant (0.9); λ is the wavelength of X-ray

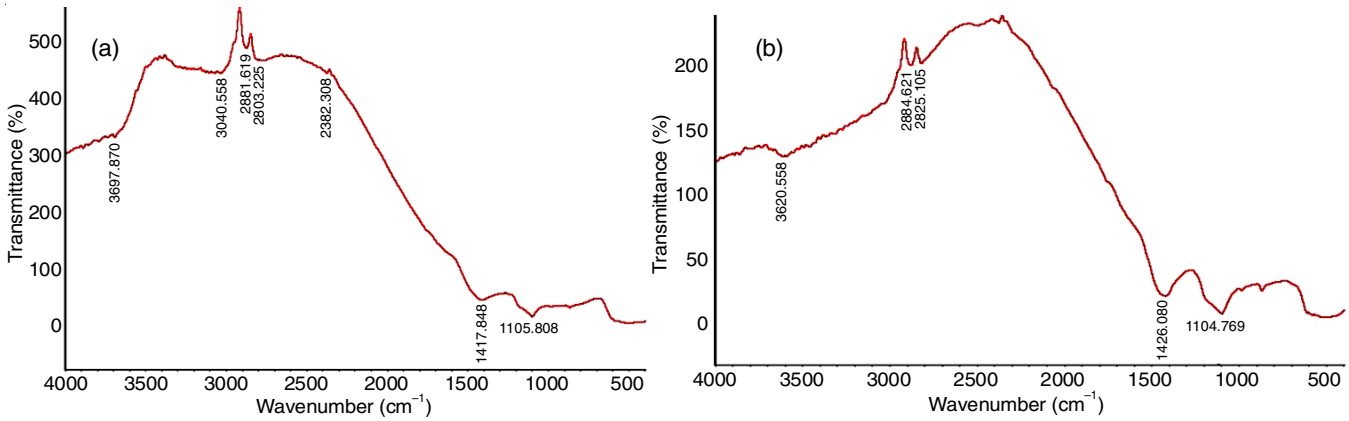

Fig. 4. FTIR spectra of CuO-carrageenan synthesized from brown strain (CuO-CRGb) (a) and green strain (CuO-CRGg) (b)

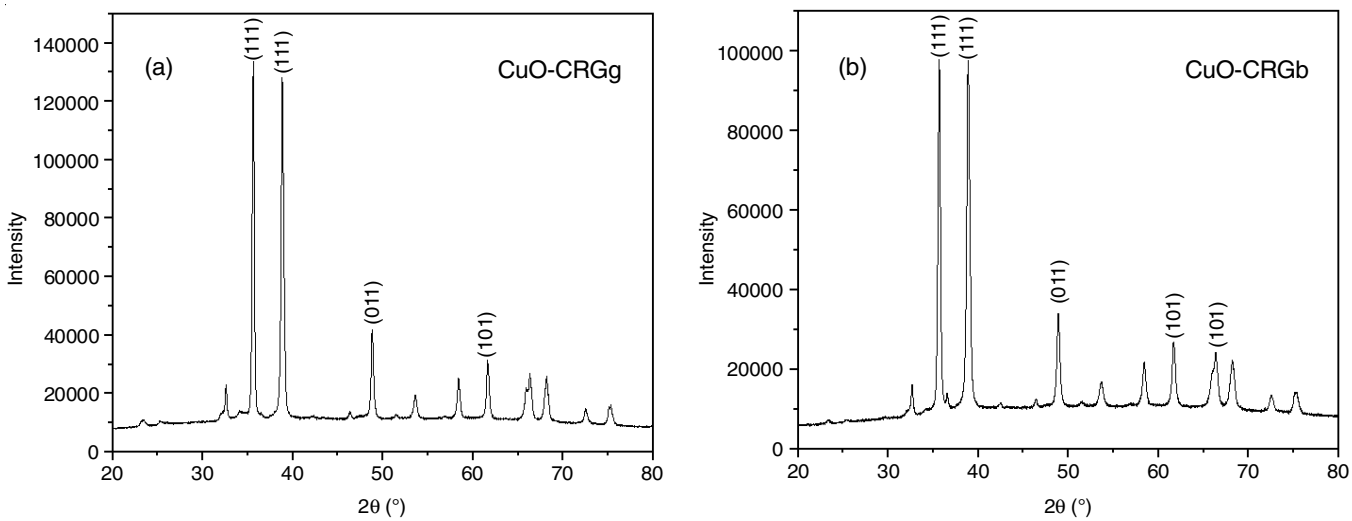

Fig. 5. X-ray diffraction peaks for (a) CuO-CRGg and (b) CuO-CRGb

radiation used and β is the FWHM of the diffraction peak in radian.

The diffraction peak acquired exhibits intensities at the angles (2θ values) of 35.61º, 38.81º, 48.82º and 61.62º for CuO-CRGg and 35.67º, 38.88º, 48.89º, 61.64º and 66.35º for CuO-CRGb (Fig. 5). After incorporating the specified relevant parameters, the analysis provides average crystalline sizes of 26 and 27 nm for CuO-CRGg and CuO-CRGb, respectively.

Photocatalytic degradation studies of methylene blue dye: The CuO-CRGb nanoparticles exhibits an efficiency of 89.76% under UV light and 55.21% under visible light, whereas CuO-CRGg nanoparticles shows 86.87% efficiency under UV light and 64.38% under visible light (Fig. 6a). The rate constants for CuO-CRGb (UV) and CuO-CRGg (UV) are 0.035 min^{-1} and 0.033 min^{-1}, respectively, with corresponding half-lives of 4.04 min and 4.12 min. Under visible light, the CuO-CRGg and CuO-CRGb nanoparticles exhibit the rate constants of 0.016 min^{-1} and 0.011 min^{-1}, with half-lives of 4.82 min and 5.15 min, respectively. Thus, it is observed that CuO-CRGb nanoparticles demonstrated a higher photocatalytic degradation efficiency of against methylene blue (10 ppm) under UV light exposure than sunlight. As the time interval increases, copper oxide nanoparticles reduce the concentration of methylene blue dye under both UV and visible light conditions. Fig. 6b illustrates that CuO-CRGb & CuO-CRGb exhibited a drastic degradation just after 20 min at UV light exposure. In context of methylene blue dye degradation, the first-order kinetics describe a reaction where the rate of degradation is directly proportional to the concentration of methylene blue dye. The degradation rate is characterized by a rate constant (k) and the process is independent of the initial concentration of methylene blue. A higher rate constant signifies a faster degradation rate.

The rate constant and half life of methylene blue dye degradation were calculated through the following equations and depicted in Table-1:

$$\ln C_t = \ln C_o - k_t \quad (2)$$

$$t_{1/2} = \ln 2/k \quad (3)$$

TABLE-1
REACTION RATES AND HALF-LIVES OF CuO-CRGg AND CuO-CRGb UNDER UV AND VIS SUNLIGHT

Nanoparticles	Rate constant (min^{-1})	Half life (min)
CuO-CRGb (UV)	0.035	4.04
CuO-CRGg (UV)	0.033	4.12
CuO-CRGg (VIS)	0.016	4.82
CuO-CRGb (VIS)	0.011	5.15

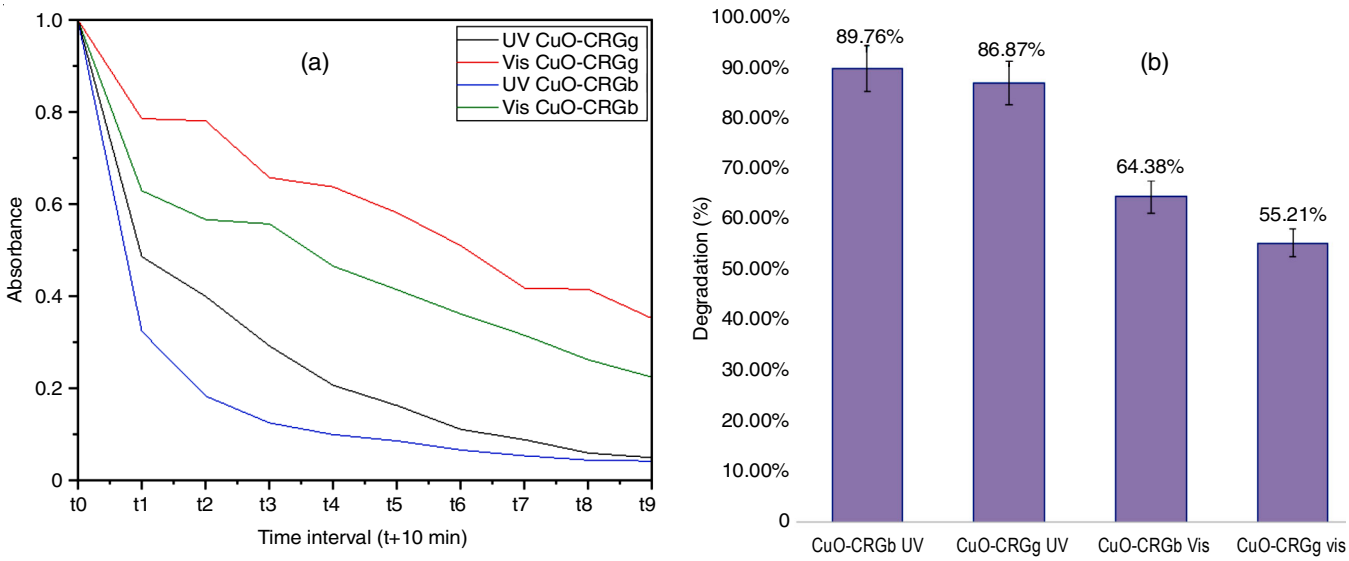

Fig. 6. Comparison of concentration decrease in methylene blue with respect to time interval change (a) and degradation efficiency (b) for CuO-CRGg and CuO-CRGb under UV and VIS light

The graph plotted with the equation data on the change in concentration of methylene blue dye over time and light conditions provided in Fig. 7 helped to analyze the kinetics of the reaction. By the obtained linear graph suggests the reaction in a first-order kinetics model, which describes the relationship between the concentration of a reactant and time. By plotting the natural logarithm of the ratio of concentration at each time point to the initial concentration [$\ln(C_t/C_o)$] against time, also obtained linear relationships for the photocatalytic activity of both CuO-CRGg and CuO-CRGb nanoparticles under UV and visible light conditions (Fig. 8). The obtained linear equations, such as $y = -0.7288x + 10.449$, where y represents $\ln(C_t/C_o)$ and x represents time, exhibit high correlation coefficients ($R^2 = 0.9915$) indicating a good fit to the first-order kinetics model. This suggests that the degradation of CuO nanoparticles follows

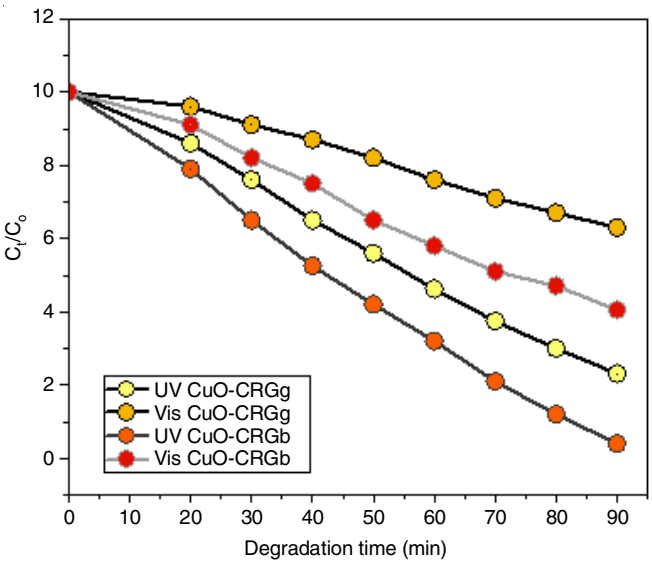

Fig. 7. Linear relationships between C_t/C_o and degradation time for CuO-CRGg and CuO-CRGb samples under UV and visible light conditions

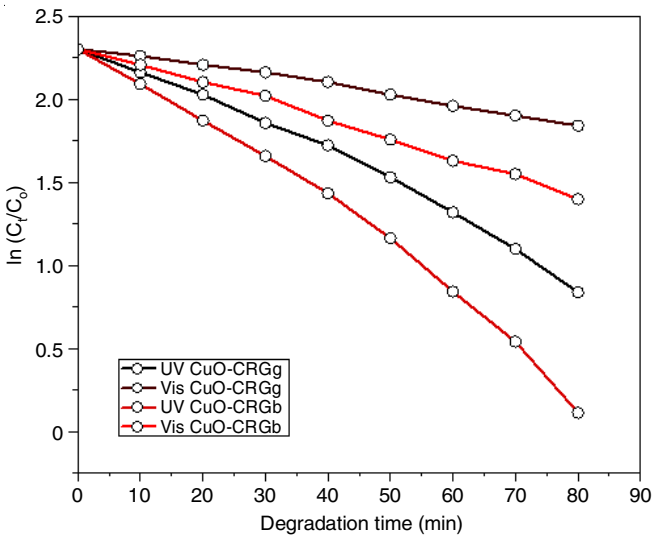

Fig. 8. Linear relationships between $\ln (C_t/C_o)$ and degradation time for CuO-CRGg and CuO-CRGb samples under UV and visible light conditions

first-order kinetics, where the rate of reaction is proportional to the concentration of the reactant. As the concentration decreases over time, the rate of degradation also decreases proportionally. Moreover, the negative slope of the linear equations implies that the concentration of CuO nanoparticles decreases exponentially over time. This behaviour is the characteristic of first order reactions, where the rate of reaction decreases exponentially as the concentration of the reactant decreases.

The photocatalytic activity of the nanoparticles against dyes are found to influenced by the morphology, crystalline structure and dimensions of nanoparticles. The CuO-CRGb having larger average particle and crystalline sizes exhibits improved photocatalytic activity under UV and sunlight. The effectiveness of CuO-CRGb catalyst is influenced by size related properties, where larger sizes enhance light absorption and improve charge carrier separation, thereby increasing photo-

TABLE-2
COMPARATIVE ANALYSIS ON PREVIOUSLY REPORTED STUDIES AND PRESENT STUDIES ON PHOTOCATALYTIC EFFICIENCY OF DIFFERENT CuO NANOPARTICLES SYNTHESIZED BY DIFFERENT METHODS AND VARYING REACTION PARAMETERS

Catalyst	Method of synthesis	Morphology	Light condition	Catalyst mass	Reaction time (min)	Degradation efficiency	Ref.
CuO	Solvothermal	Cubic shape crystal Bud shape crystal	Visible	50 mg	120	78% 61%	[27]
CuO-SDS	Precipitation	Grain like sheet	Visible	3 mg	10	100%	[28]
Cu_2O	Reduction process	Spherical shape	Visible	15 mg	15	83%	[29]
Cu-reduced GO	Absorbtion method	Spherical shape	UV + visible light	20 mg	50	94%	[30]
Cu-Al_2O_3	Impregnation,homogenized precipitation and reduction	Crystal shape	Visible light	5 mg	60	75%	[31]
Cu/CuO reduced GO	Photo reduction method	Nanorod- Flower like	UV light	20 mg	60	99.40%	[32]
CuO	Surfactant assistant	Broken flower shape	Halogen light	20 mg	30	82%	[33]
Cu_2O-Carrageenan	Sol-gel method	Agglomerate oval shape	UV light	50 mg	60	89.76%	Present Study

catalytic efficiency. The incorporation of carrageenan enhances the photocatalytic performance due to the presence of sulfate groups and morphological properties of the polymer under different light exposures. Comparing the results of the present study with those of reported works, Table-2 summarizes the photocatalytic efficiency of the synthsized CuO nanoparticles using different methods and varied reaction conditions.

Conclusion

In this work, the synthesis of CuO nanoparticles within carrageenan matrices derived from *Kappaphycus alvarezii* strains provides the valuable insights into their optical, morphological and structural properties. The variations in the absorption peaks clearly indicate size and structural differences between CuO-CRGg and CuO-CRGb. The SEM analysis confirms nanocomposite agglomeration with favourable average particle sizes for the photocatalytic applications. EDX data revealed a near stochiometric ratio of oxygen and copper weight percentages in the synthesized CuO nanoparticles. The FTIR spectra revealed the presence of carrageenan constituents and XRD analysis elucidates the crystalline arrangement in both types of the carrageenan based CuO nanoparticles. The photocatalytic degradation of methylene blue dye demonstrates the superior efficiency of CuO-CRGb under UV light, influenced by its larger particle and crystalline sizes. The study underscores the importance of the size-related properties in enhancing photocatalytic activity and suggests the potential of green synthesized nanocomposites for the environmental applications.

CONFLICT OF INTEREST

The authors declare that there is no conflict of interests regarding the publication of this article.

REFERENCES

1. R. Xiong, A.M. Grant, R. Ma, S. Zhang and V. Tsukruk, *Mater. Sci. Eng. Rep.*, **125**, 1 (2018); https://doi.org/10.1016/j.mser.2018.01.002
2. M.D. Arif, M.E. Hoque, M.Z. Rahman and M.U. Shafoyat, *Mater. Today Commun.*, **40**, 109335 (2024); https://doi.org/10.1016/j.mtcomm.2024.109335
3. T.M. Joseph, D.K. Mahapatra, A. Esmaeili, L. Piszczyk, M.S. Hasanin, M. Kattali, J. Haponiuk and S. Thomas, *Nanomaterials*, **13**, 574 (2023); https://doi.org/10.3390/nano13030574
4. S.A. Qamar, M. Junaid, A. Riasat, M. Jahangeer, M. Bilal and B.Z. Mu, *Stärke*, **76**, 2200018 (2022); https://doi.org/10.1002/star.202200018
5. C.J. Dawes, A.O. Lluisma and G.C. Trono, *J. Appl. Phycol.*, **6**, 21 (1994); https://doi.org/10.1007/BF02185899
6. M.S. Khan, S. Ranjani and S. Hemalatha, *Mater. Chem. Phys.*, **282**, 125985 (2022); https://doi.org/10.1016/j.matchemphys.2022.125985
7. Y.P. Yew, K. Shameli, M. Miyake, N. Kuwano, N.B.B.A. Khairudin, S.E.B. Mohamad and K.X. Lee, *Nanoscale Res. Lett.*, **11**, 276 (2016); https://doi.org/10.1186/s11671-016-1498-2
8. Y.P. Yew, K. Shameli, S.E.B. Mohamad, Y. Nagao, S.-Y. Teow, K.X. Lee and E.D. Mohamed Isa, *Int. J. Pharm.*, **572**, 118743 (2019); https://doi.org/10.1016/j.ijpharm.2019.118743
9. M. Sathish, T. Gobinath, A. Sundaramanickam, K. Saranya, A. Nithin and P. Surya, *Inorg. Nano-Metal Chem.*, **52**, 734 (2022); https://doi.org/10.1080/24701556.2021.1952243
10. H.N. Jayasimha, K.G. Chandrappa, P.F. Sanaulla and V.G. Dileepkumar, *Sens. Int.*, **5**, 100254 (2024); https://doi.org/10.1016/j.sintl.2023.100254
11. E. Ye and X.J. Loh, *Aust. J. Chem.*, **66**, 997 (2013); https://doi.org/10.1071/CH13168
12. M.J. Curri, R. Comparelli, P.D. Cozzoli, G. Mascolo and A. Agostiano, *Mater. Sci. Eng. C*, **23**, 285 (2003); https://doi.org/10.1016/S0928-4931(02)00250-3
13. A. Ajmal, I. Majeed, R.N. Malik, H. Idriss and M.A. Nadeem, *RSC Adv.*, **4**, 37003 (2014); https://doi.org/10.1039/C4RA06658H
14. A. Houas, H. Lachheb, M. Ksibi, E. Elaloui, C. Guillard and J.M. Herrmann, *Appl. Catal. B*, **31**, 145 (2001); https://doi.org/10.1016/S0926-3373(00)00276-9
15. I. Khan, K. Saeed, I. Zekker, B. Zhang, A.H. Hendi, A. Ahmad, S. Ahmad, N. Zada, H. Ahmad, L.A. Shah, T. Shah and I. Khan, *Water*, **14**, 242 (2022); https://doi.org/10.3390/w14020242
16. R. Sankar, P. Manikandan, V. Malarvizhi, T. Fathima, K.S. Shivashangari and V. Ravikumar, *Spectrochim. Acta A Mol. Biomol. Spectrosc.*, **121**, 746 (2014); https://doi.org/10.1016/j.saa.2013.12.020
17. C. Chen, Z. Xu, J. Qiu, W. Ye, X. Xu, R. Wang, C. Hu, J. Zhuang, B. Lei, W. Li, X. Zhang, G. Hu and Y. Liu, *ACS Appl. Nano Mater.*, **5**, 9140 (2022); https://doi.org/10.1021/acsanm.2c01444
18. K. Atacan, B. Topaloglu and M. Özacar, *Appl. Catal. A Gen.*, **564**, 33 (2018); https://doi.org/10.1016/j.apcata.2018.07.020

19. B. Belache, Y. Khelfaoui, M. Bououdina, T. Souier and W. Cai, *J. Lumin.*, **207**, 258 (2019); https://doi.org/10.1016/j.jlumin.2018.11.029
20. C.H. Ashok, K.V. Rao and C.S. Chakra, *J. Atoms Mol.*, **4**, 803 (2014).
21. E. Ayoman and S.G. Hosseini, *J. Therm. Anal. Calorim.*, **123**, 1213 (2016); https://doi.org/10.1007/s10973-015-5059-1
22. A.A. Oun and J.W. Rhim, *Food Hydrocoll.*, **67**, 45 (2017); https://doi.org/10.1016/j.foodhyd.2016.12.040
23. S. Jacob, A.B. Nair, J. Shah, S. Gupta, S.H.S. Boddu, N. Sreeharsha, A. Joseph, P. Shinu and M.A. Morsy, *Pharmaceutics*, **14**, 533 (2022); https://doi.org/10.3390/pharmaceutics14030533
24. K. Tharani and L.C. Nehru, *Rom. J. Biophys.*, **30**, 55 (2020).
25. R.M. Amir, F.M. Anjum, M.I. Khan, M.R. Khan, I. Pasha and M. Nadeem, *J. Food Sci. Technol.*, **50**, 1018 (2013); https://doi.org/10.1007/s13197-011-0424-y
26. N. Hans, S. Gupta, F. Pattnaik, A.K. Patel, S. Naik and A. Malik, *Int. J. Biol. Macromol.*, **250**, 126230 (2023); https://doi.org/10.1016/j.ijbiomac.2023.126230.
27. G. Sorekine, G. Anduwan, M.N. Waimbo, H. Osora, S. Velusamy, S. Kim, Y.S. Kim and J. Charles, *J. Mol. Struct.*, **1248**, 131487 (2022); https://doi.org/10.1016/j.molstruc.2021.131487
28. N. Benhadria, M. Hachemaoui, F. Zaoui, A. Mokhtar, S. Boukreris, T. Attar, L. Belarbi and B. Boukoussa, *J. Cluster Sci.*, **33**, 249 (2022); https://doi.org/10.1007/s10876-020-01950-0
29. M. Kumar, R.R. Das, M. Samal and K. Yun, *Mater. Chem. Phys.*, **218**, 272 (2018); https://doi.org/10.1016/j.matchemphys.2018.07.048
30. B.A. Aragaw and A. Dagnaw, *Ethiopian J. Sci. Technol.*, **12**, 125 (1970); https://doi.org/10.4314/ejst.v12i2.2
31. M.J. Ndolomingo and R. Meijboom, *Appl. Catal. A Gen.*, **506**, 33 (2015); https://doi.org/10.1016/j.apcata.2015.08.036
32. B.A. Aragaw and A. Dagnaw, *Ethiop. J. Sci. Technol.*, **12**, 125 (2019); https://doi.org/10.4314/ejst.v12i2.2
33. M.P. Rao, S. Anandan, S. Suresh, A.M. Asiri and J.J. Wu, *Energy Environment Focus*, **4**, 250 (2015); https://doi.org/10.1166/eef.2015.1168